Air-Sea Gas Fluxes Using Altimeter-Derived Gas Transfer Velocities in an Ocean General Circulation Model

David M. Glover[1], Nelson M. Frew[1], Scott C. Doney[1], Ivan D. Lima[1], Michael J. Caruso[2], and Scott J. McCue[1]

[1]Woods Hole Oceanographic Institution, Woods Hole, MA 02543
[2]RSMAS University of Miami, Miami, FL 33149

Introduction

An algorithm that estimates gas transfer velocities (k) from the mean square slope of centimetric sea surface waves derived from normalized radar backscatter measured by altimeters was applied to a variant of the NCAR Community Climate System Model-Parallel Ocean Program (CCSM-POP). This ocean general circulation model includes a fully coupled marine ecosystem/carbon cycling sub-model. Historical hindcast simulations were integrated from 1958 to the beginning of 1993 using gas transfer velocities derived from NCEP reanalysis wind speeds and the Wanninkhof quadratic wind speed algorithm. Twin experiments were conducted from 1 Jan 1993 to 1 Jan 2005 using transfer velocities derived either from NCEP reanalysis winds or TOPEX data. We focus our analysis on a comparison of the time/space differences in air-sea CO_2 and O_2 fluxes and surface water pCO_2 and pO_2 (as % supersaturation) fields between the two experiments. Our objectives are to explore the sensitivity of ocean biogeochemistry to global and basin scale variations in gas transfer velocity, gain greater understanding of the global accuracy of the altimeter algorithm, and provide insight into the various processes influencing the net CO_2 and O_2 fluxes across the air-sea interface.

Ocean General Circulation Model (OGCM)

- Variant of the NCAR Community Climate System Model-Parallel Ocean Program (CCSM-POP).
- Includes a fully coupled marine ecosystem/carbon cycling sub-model.
- Coupled to full-depth ocean BGC model (CCSM-POP)
- WHOI/NCAR/Irvine multi-functional group, multi-nutrient ecosystem model (Moore *et al.*, 2004).
- Historical hindcast simulations were integrated from 1958 to the beginning of 2005 using NCEP reanalysis products.
- Surface physics forcing (1957-2004) from NCEP reanalysis and satellite products (Yeager and Large, 2004).
- Time-varying atmospheric dust/iron deposition (NCAR/MATCH simulations).
- 1 Jan 1993 a twin model run was spawned using TOPEX-derived gas transfer velocities to the beginning of 2005.
- Polar locations where there was no TOPEX orbital coverage were replaced with Wanninkhof (1992) based transfer velocities.

Gas Transfer Velocity (k)

Wind Speed Based (U_{10}) k (cm/h)

$$k = 0.31 U_{10}^2 \left(\frac{Sc}{660}\right)^{-\frac{1}{2}}$$

Wanninkhof (1992)

Altimeter Based (TOPEX) k (cm/h)

$$k = C_0 + C_1 \left(\Delta\left\langle s^2\right\rangle_{40}^{100}\right)^2 \left(\frac{Sc}{660}\right)^{-\frac{1}{2}}$$

Frew *et al.* (2007)

The $\Delta\left\langle s^2\right\rangle_{40}^{100}$ is estimated from altimeter data:

$$\Delta\left\langle s^2\right\rangle_{40}^{100} = \left(\frac{\rho'_{Ku}}{\sigma^\circ_{Ku}} - \frac{\rho'_C}{(\sigma^\circ_C + \alpha)}\right)$$

Frew *et al.* (2007)

where:

- U_{10} = wind speed at 10m elevation from the sea surface,
- Sc = the Schmidt number, which is a function of temperature and salinity,
- $\Delta\left\langle s^2\right\rangle_{40}^{100}$ = the differenced mean square slope, evaluated between wavenumbers of 40 and 100 rad/m,
- C_0, C_1 = empirical constants determined from field data,
- ρ'_{Ku}, ρ'_C = effective reflectivity for nadir looking radar at Ku and C bands,
- $\sigma^\circ_{Ku}, \sigma^\circ_C$ = altimeter normalized radar backscatter at Ku and C bands,
- α = an *ad hoc* adjustment to C-band σ°_C allowing for the lack of absolute C-band backscatter calibration.

Twin Experiment Output

Model output using the Wanninkhof (1992) relationship between wind speed and gas transfer velocity will be referred to as **Reference runs** and, when shown, will be shown first. Model output differing from the reference run only by using the radar backscatter-based estimates of k will be referred to as **TOPEX k runs** and will be shown second. The difference between these two runs will always be reference run minus TOPEX k run and will be shown third. Furthermore, due to the nature of the manipulations necessary to interpolate TOPEX data (10-day exact repeat orbit) to the 6-hourly model T62 grid, all results are displayed on a seasonal basis. We have adopted the following convention for our seasonal time series with winter (Jan, Feb, Mar), spring (Apr, May, Jun), summer (Jul, Aug, Sep), and autumn (Oct, Nov, Dec).

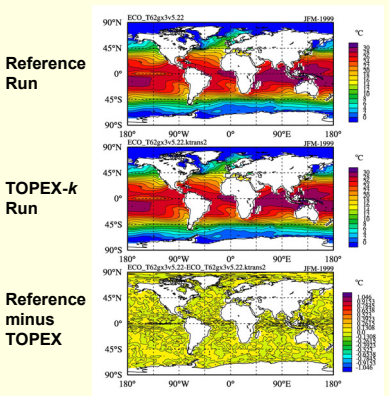

Figure 1. Global Temperature Fields for TOPEX and Reference Runs

- The reference case, OGCM is integrated with all the usual forcings and parameterizations. This is the global temperature field for winter (Jan, Feb, Mar) of 1999.
- The global temperature field for winter 1999 with everything the same as the reference case above, *except* that the gas transfer velocities are derived from TOPEX normalized radar backscatter according to the algorithm explained above and in Frew *et al.* (2007).
- The difference of the above two temperature fields. Note the low magnitude, random, featureless distribution of positive and negative differences, implying that the change of transfer velocities had no dynamic effect on the OGCM integration.

Results

The seasonal global gas transfer velocity fields for the year 1999 for the twin experiments are compared in Figure 2 below. These are reported for Sc = 660, i.e. for a surface ocean at a uniform 20°C. The Wanninkhof transfer velocities are generally higher than those computed from TOPEX.

Figure 2. Global Gas Transfer Velocity k (Sc = 660) for Year 1999

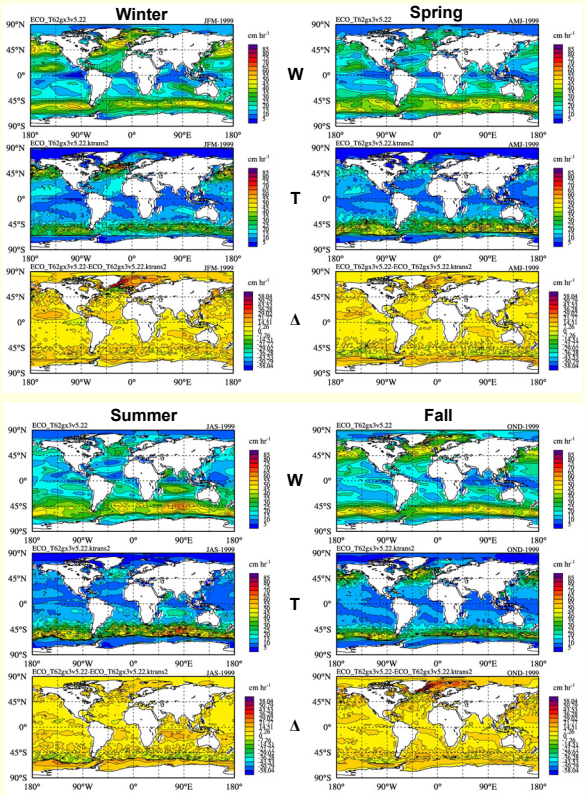

In computing gas fluxes, the transfer velocity fields are further adjusted for the variation of Sc with temperature and salinity using the OGCM's dynamic fields for these properties. Figure 3 shows the global CO_2 and O_2 fluxes for the northern hemisphere wintertime of the same year. The fluxes for the twin experiments are similar; the fluxes agree to within 0.65 mol m^{-2} y^{-1} for CO_2 and 5 mol m^{-2} y^{-1} for O_2. Larger differences in the CO_2 flux are notable in the western equatorial Pacific and along 45°S in the Atlantic sector of the Southern Ocean. The latter region is of interest because it is the proposed site of the next major gas exchange field experiment, GasEx-3 (URL (2007)).

Figure 3. Global CO_2 and O_2 Fluxes for Northern Wintertime 1999

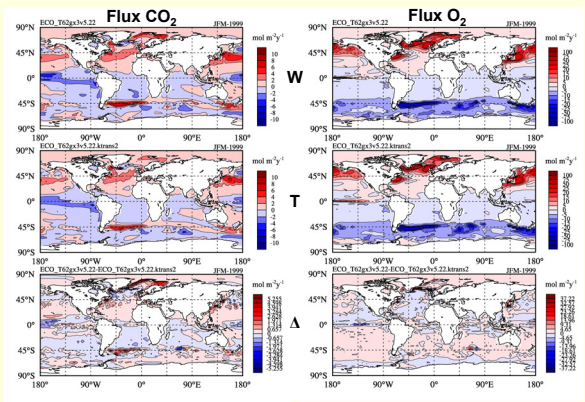

The model runs shown in Figure 3 are for the pre-industrial atmospheric CO_2 level (278 ppmv), which serves as a baseline against which the results for current atmospheric levels (380 ppmv) including the accumulated anthropogenic CO_2 input can be compared. Figure 4 shows the predicted 11-year time series (1993-2004) of global surface fluxes of CO_2 and O_2 for the reference and TOPEX pre-industrial runs. The net global average yearly fluxes for the TOPEX era are -1.5 Pg-O_2 y^{-1} and +0.13 Pg-C y^{-1} (ref. run) and -2.4 Pg-O_2 y^{-1} and -0.04 Pg-C y^{-1} (TOPEX run). Preliminary estimates of the anthropogenic run fluxes are -1.3 Pg-O_2 y^{-1} and +1.8 Pg-C y^{-1} (reference) and -1.3 Pg-O_2 y^{-1} and +1.6 Pg-C y^{-1} (TOPEX). The carbon flux estimates are consistent with a recent estimate (1.3 ± 5 Pg-C y^{-1}) reported by Sweeney *et al.* (2007) based on revised oceanic bomb ^{14}C inventories. Older estimates cited in Sweeney *et al.*, 2007) range from 1.8-2.4 Pg-C y^{-1}.

Figure 4. Time Series of Global Surface CO_2 and O_2 Fluxes

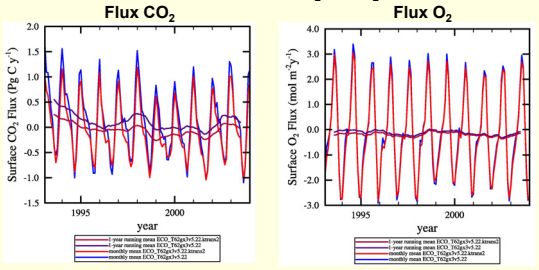

Regional Comparison - Southern Ocean

The partitioning of biologically and climatically important gases between the surface ocean and the atmosphere is controlled by the complex interaction of multiple processes, including biological production and consumption within the water column, solubility and diffusivity changes driven by temperature and salinity variations, vertical/horizontal advection, and direct and bubble-mediated gas transfer across the air–sea interface. The relative importance of these processes varies both spatially and temporally. We use an OGCM to simulate complex processes of physical kinematics, biological activity and dynamic circulation that interact with each other to determine the net gas flux between the ocean and atmosphere.

In order to understand different influences on the net flux of CO_2 and O_2 between the ocean and atmosphere, we have examined variations in model output in terms of differences of transfer velocities (Δk), surface saturation (ΔSSAT) and gas flux (ΔF). The following figures compare reference and TOPEX-k runs for CO_2 and O_2 in the north Southern Ocean sub-region of the OGCM (30°S – 55°S) during the austral summer, when biological activity is drawing down surface CO_2 and producing O_2.

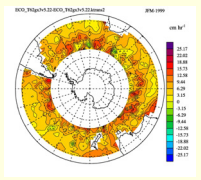

Table 1: Prediction of ΔFlux

	Δk +		Δk –	
	ΔSSAT +	ΔSSAT –	ΔSSAT +	ΔSSAT –
+ $SSAT_W$ F↑– + $SSAT_T$ F↑–	$F_W \ll F_T$ ΔF –	$F_W \gtrless F_T$ ΔF ±	$F_W \leq F_T$ ΔF ±	$F_W \gg F_T$ ΔF +
+ $SSAT_W$ F↑– – $SSAT_T$ F↓+	$F_W \ll F_T$ ΔF –		$F_W \ll F_T$ ΔF –	
– $SSAT_W$ F↓+ + $SSAT_T$ F↑–		$F_W \gg F_T$ ΔF +		$F_W \gg F_T$ ΔF +
– $SSAT_W$ F↓+ – $SSAT_T$ F↓+	$F_W \leq F_T$ ΔF ±	$F_W \gg F_T$ ΔF +	$F_W \ll F_T$ ΔF –	$F_W \gtrless F_T$ ΔF ±

Figure 5. Δk (W-T) for north Southern Ocean sub-region

Figure 5 shows that the reference run transfer velocities are overall larger than the TOPEX-derived k in the north Southern Ocean (Δk are largely positive).

Table 1 shows the contingency for determining the sign of the flux difference using either Wanninkhof (1992) or Frew *et al.* (2007) to calculate k in the OGCM (Moore *et al.*, 2004). The table is divided into 16 difference cells depending whether Δk ($k_W - k_T$) is positive *i.e.,* transfer velocity from Wanninkhof is greater than Frew *et al.* or vice versa and whether the surface saturation is positive or negative and their difference. In Table 1, W is for Wanninkhof (1992), T refers to TOPEX (Frew *et al.*, 2007), k is the transfer velocity, SSAT is the surface saturation of the gas, F is the flux of the gas with the model convention that flux into the ocean is positive and the colors are to guide the eye to where the difference should be positive (red) or negative (blue). At times and in certain locations, the indicators are contrary and the flux difference could be either positive or negative (colored green).

Figure 6. Surface O_2 and CO_2 Saturations and Fluxes for north Southern Ocean

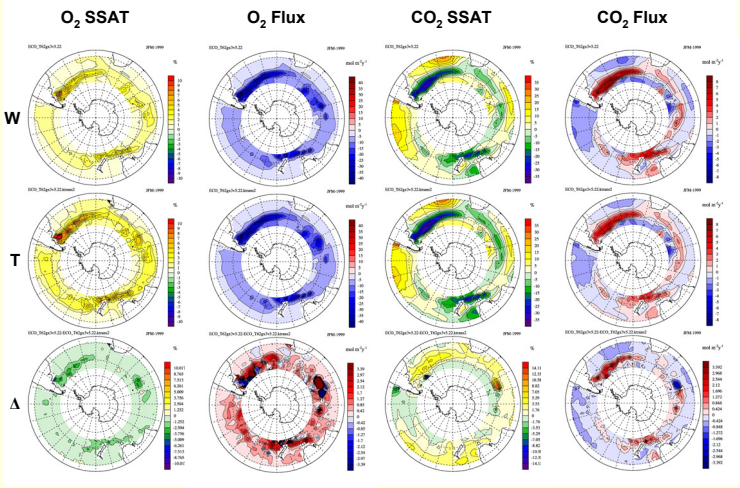

In Figure 6, the O_2 surface saturations are positive for both the reference and TOPEX derived k's, with some intensified regions particularly in the area of the proposed GasEx-3 site, while the CO_2 surface saturations are of the opposite sign in those regions. Combination of Table 1 with Figs. 5 and 6 predict the direction of the flux of these gases in the north Southern Ocean. The differences in the fluxes are largely of the same sign in these intense regions in spite of the fact that the saturation differences have opposite signs, demonstrating the importance of both the magnitude and direction of the contributing processes. These differences are *model* differences; field data from the planned GasEx-3 campaign are needed to explore and verify potential underlying processes.

Examination of these and other model output fields suggest a working hypothesis to explain the variety of results presented so far. In regions and at times when the patterns in differences of transfer velocities (Δk), surface saturation (ΔSSAT) and gas flux (ΔF) are positively or negatively correlated, biological activity appears to be the dominant control on the air-sea flux. But in other regions and at other times where one or all of these variables do not display any correlation, physical processes dominate the surface flux. Further study of model output and field data (e.g. GasEx-3) should help to tease apart the underlying processes and quantify their contribution to the flux. Many previous assessments of global surface CO_2 fluxes have been based on a static surface pCO_2 field. This experiment emphasizes the importance of including dynamic physical processes and a coupled biological model in computing surface gas fluxes.

References

Frew, N. M., D. M. Glover, E. J. Bock, and S. J. McCue (2007), A new approach to estimation of global air-sea gas transfer velocity fields using dual-frequency altimeter backscatter, *in review, J. Geophys. Res.*

Moore, J.K., S.C. Doney, and K. Lindsay (2004), Upper ocean ecosystem dynamics and iron cycling in a global three-dimensional model, *Global Biogeochem. Cycles, 18*, GB4028.

Sweeney, C., E. Gloor, A. R. Jacobson, R. M. Key, G. McKinley, J. L. Sarmiento, and R. Wanninkhof (2007), Constraining global air-sea gas exchange for CO_2 with recent bomb ^{14}C measurements, *Global Biogeochem. Cycles*, in press.

URL (2007), http://duck-rabbit.ldeo.columbia.edu/so_gasex

Wanninkhof, R. (1992), Relationship between wind speed and gas exchange over the ocean, *J. Geophys. Res.*, *97*, 7373-7382.

Yeager, S.G. and W.G. Large (2004), Late winter generation of spiciness on subducted isopycnals, *J. Phys.* Oceanogr., *34*, 1528-1547.